Angle-and Time-Resolved Two-Photon Photoemission Spectroscopy for Unoccupied Levels of Lead Phthalocyanine Film

ARTICLE *in* THE JOURNAL OF PHYSICAL CHEMISTRY C · AUGUST 2011

Impact Factor: 4.77 · DOI: 10.1021/jp205922q

THE JOURNAL OF PHYSICAL CHEMISTRY C

ARTICLE

pubs.acs.org/JPCC

Angle- and Time-Resolved Two-Photon Photoemission Spectroscopy for Unoccupied Levels of Lead Phthalocyanine Film

Masahiro Shibuta, Keisuke Miyakubo, Takashi Yamada, and Toshiaki Munakata*

Department of Chemistry, Graduate School of Science, Osaka University, Osaka 560-0043, Japan

ABSTRACT: We have measured angle- and time-resolved two-photon photoemission (2PPE) from unoccupied levels of graphite (HOPG) and lead phthalocyanine (PbPc) films. Our angle-resolved 2PPE microspot spectroscopy with a lateral resolution of 0.4 μm can effectively select flat and homogeneous regions of the film, allowing measurements of the dispersion of the image potential state (IPS) on the PbPc film. The effective mass of the IPS on the film is 2.2 ± 0.2, which is heavier than that for the bare HOPG, 1.2 ± 0.1. The lifetimes of the states at 30 K are 30 fs for both the HOPG and the PbPc film. These results suggest a hybridization of the IPS with a molecule-derived unoccupied level. The lifetimes of the lowest unoccupied molecular level (LUMO)-derived levels are about 80 fs. A possible decay process to lower states is suggested.

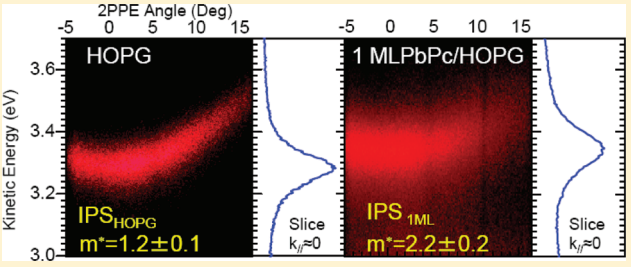

1. INTRODUCTION

The electronic structures of organic thin films have been extensively investigated in the past few decades, from the perspectives of both fundamental science and advanced technology. The functionality of organic films is frequently discussed on the basis of photoemission and inverse photoemission results.[1−5] Photoemission experiments provide rich information on the electronic structures as well as on the dispersions of the occupied bands. On the other hand, experiments on unoccupied bands, which play a crucial role in electron transportation, are still challenging.[6,7] Two-photon photoemission (2PPE) spectroscopy, in which a normally unoccupied level is populated by a first photon and the excited electron is probed by photoemission with the second photon, is a powerful method to detect unoccupied levels.[8,9] By scanning the delay time between the pump and probe pulses, the time evolution of the excited state is detected with femtosecond time resolution. The dispersion of the unoccupied band can be measured by an angle-resolved (AR) photoemission method. An especially severe problem for organic films is the lateral inhomegeneity of the film. Organic films typically grow with lateral inhomegeneity, and the inhomogeneity causes the complexity of the electronic structure.[10−12] The lateral inhomogeneity strongly affects the angular distribution of the photoelectrons,[13] hampering reliable measurement of the dispersion of unoccupied bands. In some cases, AR measurement is made by simply rotating the sample. The probe area is changed by the rotation, and it is not possible to selectively probe an uniform area on the film. Such AR results are not very reproducible when the films are nonuniform. This situation occurs for lead phthalocyanine (PbPc) films formed on highly oriented pyroritic graphite (HOPG). Although these films seem uniform when observed by a photoemission electron microscope with resolution of 50 nm,[12] they are not uniform at the nanometer scale.[11] This nonuniformity significantly affects the AR measurement of these films. In this work, we have extended our microspot 2PPE spectrometer[11,14,15] to AR experiments, and the performance is tested for PbPc films on HOPG. Previously, we assigned the molecule-derived energy levels in the PbPc films due to the highest occupied molecular orbital (HOMO), the next HOMO (HOMO-1), and the lowest unoccupied molecular orbital (LUMO), LUMO+1, LUMO+2, and the first image potential state (IPS).[14] The well-analyzed system is suitable for developing further understanding of the unoccupied states at the substrate−molecule interfaces by extending the 2PPE experiment to AR and time-resolved (TR) modes. We demonstrate that the dispersion of the IPS on the film can be successfully measured by selecting a uniform area of the one monolayer (1 ML) PbPc film. By combining with TR experiments, the interaction of the IPS with a higher-lying molecular orbital, presumably LUMO+3, is discussed. The lifetimes and decay processes of LUMO- and LUMO+1-derived levels are also discussed.

2. EXPERIMENTAL METHODS

The microspot AR-2PPE experiments are performed in a newly constructed apparatus partly similar to that reported previously.[11,14,15] The light source is the *p*-polarized third harmonic output of a tunable titanium sapphire laser (Coherent: Mira-900F) operated at a pulse duration of 100 fs and a repetition of 76 MHz. All measurements are performed with one-color 2PPE. The light is focused onto the sample with a Schwarzschild objective of 0.29 numerical aperture. The spot size on the sample surface is about 0.6 μm and achieves a lateral resolution of 0.4 μm

Received: June 23, 2011
Revised: August 23, 2011
Published: August 29, 2011

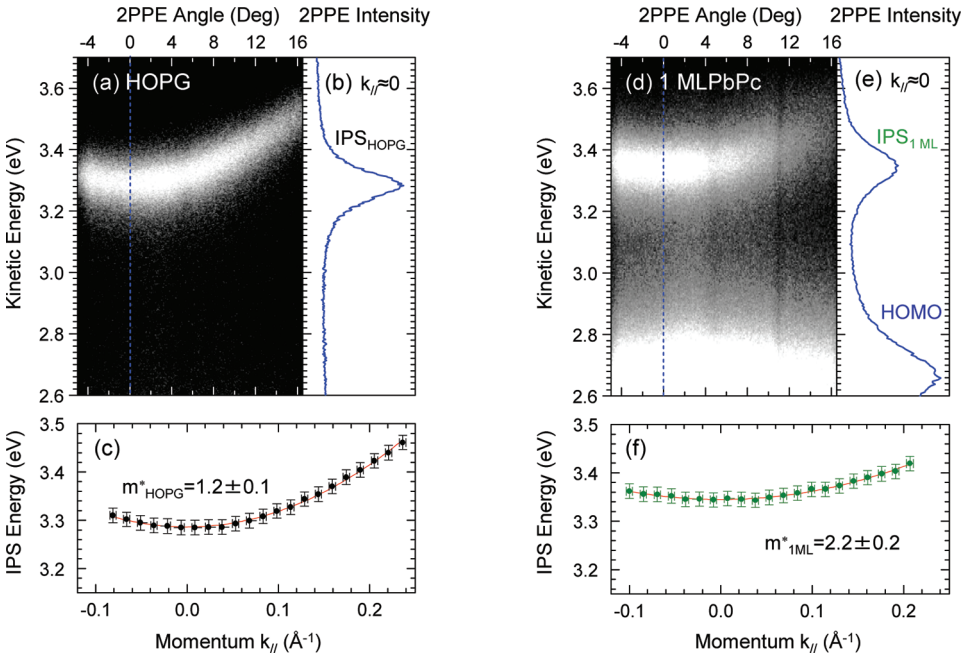

Figure 1. Angle-resolved microspot 2PPE results for HOPG (left panels) and the 1 ML PbPc film (right panels) measured with 4.13 eV photon energy. (a) Angle data for HOPG, (b) its slice around 0°, and (c) the peak energy plotted against $k_{//}$. By parabolic fitting, the effective mass of IPS on HOPG is 1.2 ± 0.1. (d) Angle data for the PbPc film, (e) a slice around 0°, and (f) the dispersion of the IPS on the PbPc film. The effective mass is 2.2 ± 0.2. No dispersion is detected for the HOMO band.

in 2PPE experiments.[11,14,15] The sample is grounded, and photoelectrons are detected with an angle-resolved hemispherical energy analyzer (VGSCIENTA: R-3000). It is confirmed that the AR results measured with different rotation angles of the sample connect smoothly with each other. TR-2PPE experiment is performed using a different apparatus equipped with another hemispherical energy analyzer (VG: CLAM4) with nine channeltron detectors.[16,17] The pulse width of the laser output is reduced to 50 fs by removing the birefregent filter normally installed in Mira-900F cavity. After compressing the third harmonic output with a pair of fused silica prisms, the pulse width is about 70 fs, as determined by fitting to a Gaussian autocorrelation function. The pump and probe pulses are directed to the surface with a skewed configuration to remove interference between the pulses. The diameter of the light spot at the sample surface is about 80 μm. The HOPG substrate was cleaved in air and cleaned by heating at 673 K for 50 h in UHV. The cleanliness was confirmed by the work function (4.45 eV) and the peak width of the IPS feature (<140 meV) measured with 2PPE spectroscopy.[14,16,17] PbPc films of 1 ML coverage were prepared by annealing films of 0.4 nm thickness (reading of a quartz microbalance) at 373 K for 1 h.[12,14]

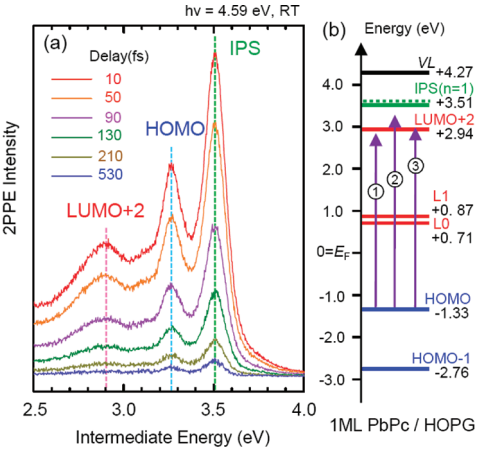

Figure 2. (a) Time-resolved 2PPE spectra measured at the photon energy of 4.59 eV. The peak positions and widths show no significant delay-time dependence. (b) Energy level diagram for the PbPc film.[17] The broken dark green line shows the IPS for clean HOPG. The vertical arrows labeled 1, 2, and 3 indicate the photon energies for Figures 1, 2, and 4, respectively.

3. RESULTS AND DISCUSSION

3.1. Angular Distribution. Figure 1a shows an angular distribution of photoelectrons from the first IPS on the clean HOPG substrate. The horizontal and vertical axes are the photoemission angle θ with respect to the surface normal and the kinetic energy E_k, respectively. The trace in Figure 1b is the spectrum integrated over the angle region of ±0.92°. The binding energy of the IPS with respect to the vacuum level (VL) is 0.85 eV. Figure 1c shows the kinetic energy of the IPS peak as a function of the electron wavenumber parallel to the surface ($k_{//}$) defined by $k_{//} = (2m_eE_k/\hbar^2)^{1/2}\sin\theta$ where m_e is the mass of a free electron. The effective electron mass ratio m^*/m_e in the IPS is evaluated to be 1.2 ± 0.1 by fitting to a parabolic function of $E_k = \hbar^2k_{//}^2/2m^*$. The value reproduces the inverse photoemission results[18] with higher resolution. Measurements with the microspot (0.4 μm) and conventional (80 μm) configurations give essentially the same results.

Figures 1d–f show the AR-2PPE results for the 1 ML PbPc film. The 2PPE measurements shown in Figure 1a,d are performed with the photon energy of 4.13 eV. The photon energy is selected so that the IPS on PbPc film is not resonantly enhanced

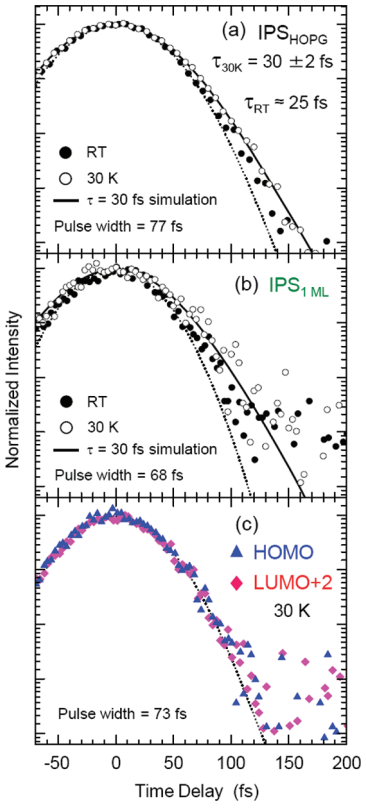

Figure 3. Decay of (a) IPS on clean HOPG, (b) IPS on the 1 ML PbPc film, and (c) HOMO and LUMO+2 peaks. The dotted line is the Gaussian autocorrelation function of the pulse width indicated at the left bottom of each panel. The lifetimes for RT are slightly shorter than that at 30 K for a and b. The lifetime of LUMO+2 is too short to be determined.

by the transition from the HOMO-derived level. The photon energy is below the resonance between the HOMO and the LUMO+2-derived levels (see Figure 2b).[16,17] The IPS's shown in Figure 1 are excited from occupied bulk bands by $k_{//}$ nonconserving transitions.[17] Taking the workfunction of the film to be 4.27 eV, the IPS is located 0.78 eV below the VL. The effective mass is evaluated to be 2.2 ± 0.2 by the parabolic fitting. The effective mass is significantly heavier than that for the clean surface. Note that the dispersion measured with a conventional 2PPE configuration is not very reproducible; for some films the spectra at high emission angles became broad, and the dispersion was not clear. Although we are very careful to form well-ordered 1 ML films as described in refs 16 and 17, the remaining inhomogeneity still affects the angular distribution of photoelectrons. The sensitivity of AR experiments to the quality of organic film is known for 3,4,9,10-perylene tetracarboxylic dianhydride (PTCDA) films.[13] As reported in refs 11 and 12, PbPc molecules do not form small crystalline domains but are randomly distributed on the HOPG surface for sub-ML films. The growth mode of the film makes the AR measurement difficult when using a large probe area. We confirmed that reproducible results, such as those shown in Figure 1d, are obtained for different samples with the microspot configuration.

The heavy effective mass suggests that the PbPc film is not a simple dielectric isolation layer. The effective mass in the IPS on rare gas or alkane films on noble metal surfaces is close to 1.[19−22] We believe that the IPS is hybridized with a molecule-derived unoccupied level, presumably the LUMO+3 derived level. Such a high-lying level around the IPS has been predicted by a density functional theory (DFT) calculation for a free molecule.[14] The electron in the IPS is then partially trapped in the molecule-derived level, increasing the effective mass. This is consistent with our former observation of the enhancement of the IPS peak by the formation of the 1 ML film.[17] The enhancement of the IPS peak suggests that the penetration of the IPS wave function into the bulk is increased by the film. Such enhanced penetration occurs when the IPS is hybridized with a molecule-derived unoccupied level.

The 2PPE signal at around 2.7 eV in Figure 1d is due to coherent 2PPE from the HOMO-derived level. It seems that the HOMO band is not dispersing or the dispersion is very weak. The details will be discussed after further experiment.

3.2. Time-Resolved Measurement. To confirm the hybridization, a time-resolved experiment is performed. Figure 2a shows normal-emission 2PPE spectra for 1 ML PbPc/HOPG measured at different delay times between the pump and the probe pulses. The photon energy of 4.59 eV is slightly above the resonance between the HOMO and the LUMO+2 derived levels as shown in the energy level diagram of Figure 2b.[16,17] The HOMO and LUMO+2 derived levels appear as clearly separated peaks. The spectra in Figure 2a are obtained by subtracting the spectrum at the time delay of 24 ps from the spectrum at each delay time. As can be seen in Figure 2a, no significant changes in the peak positions and widths with delay time are identified. The time evolutions of the IPS peak intensities for the clean HOPG and the 1 ML PbPc film, measured at room temperature (RT) and 30 K, are plotted against the delay time in Figures 3a and b, respectively. The lifetimes (τ) are evaluated by a single-exponential decay. The lifetime of the clean IPS is estimated to be 30 and 25 fs for the sample temperatures of 30 K and RT, respectively. Although the obtained values are affected by the functional form of the autocorrelation, the shorter lifetime at higher temperature is reproducible and is in accordance with other results.[23,24]

Figure 3b shows the decay of the IPS peak on the PbPc film at RT and 30 K. The TR results for the films are not very sensitive to the probe area. The lifetime is comparable to that of the IPS on clean HOPG. When the adsorbed molecules act as a dielectric isolation layer, the lifetime of the IPS becomes longer because of the decrease in the tail component of the wave function penetrating into the substrate.[19−21] The comparable lifetimes suggest that the IPS wave function penetrates into the substrate through the molecular layer. The penetration is reasonable when we assume hybridization of IPS with the LUMO+3-derived level. The molecule-derived unoccupied level mixes with the free electron-like IPS state and forms a two-dimensional delocalized band. Thus, the lifetime is consistent with the AR-2PPE results. The lifetime of the IPS for the PbPc film at RT is slightly shorter than that at 30 K. Vibronic coupling in the electronic excited state may affect the lifetime.

The interaction of IPS with a molecular-unoccupied level was discussed for C_6F_6/Cu(111)[25,26] in which the molecular resonance peaks were largely shifted from the IPS on the substrate. Two molecular resonant states were detected, and the effective masses were about 1 and >2. The lifetimes were as short as 7 fs for the 1 ML film. The electron masses and the short lifetimes are significantly different from the present results. The IPS on the PbPc film is only slightly shifted from that on HOPG. The substrate/molecule interactions in PbPc/HOPG are different from those in C_6F_6/Cu(111).

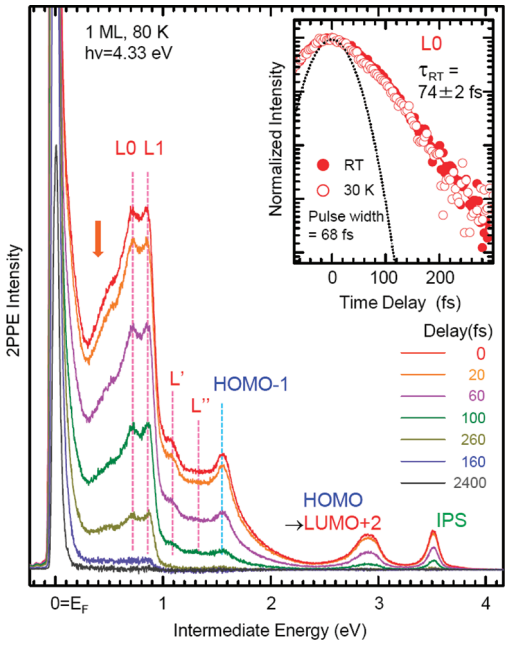

Figure 4. Time-resolved 2PPE spectra of the 1 ML PbPc film measured at the photon energy of 4.33 eV. The unassigned peaks in ref 17 are denoted L′ and L″. The inset shows that the lifetime of the L0 peak is 74 fs with no clear temperature dependence. Solid and open circles represent results for the sample temperature of RT and 30 K, respectively. The dotted line is the autocorrelation function of a 68 fs pulse width. The peak positions of L0 and L1 show no shifts. The intensity ratio between the peaks is also independent of the delay time. A shoulder is visible at 0.4 eV as indicated by the downward arrow. Low energy electrons appear in the energy region below 0.3 eV.

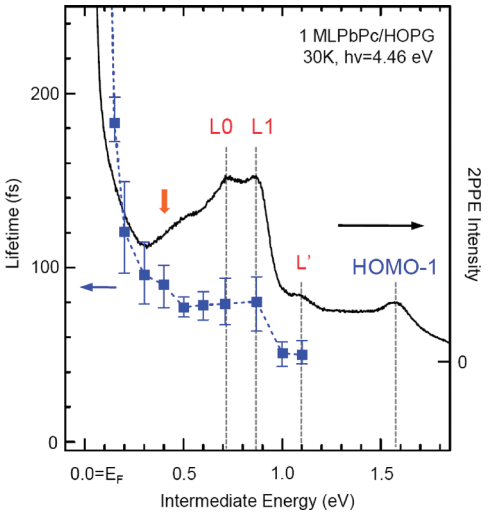

Figure 5. Lifetime measured at the photon energy of 4.46 eV compared with the 2PPE spectrum in Figure 4. The lifetimes for L0 and L1 peaks are about 80 fs. The lifetime rapidly increases at the leading edge of the L1 peak. The lifetime at 0.4 eV indicated by the downward arrow is longer than those at L0 and L1. The lifetime becomes very long at energies below 0.3 eV.

The delay time dependence of the HOMO and LUMO+2-derived peaks is shown in Figure 3c. The agreement of the time dependence of the HOMO-derived peak with the autocorrelation trace confirms the validity of the lifetime analysis. The lifetime for the LUMO+2-derived level is shorter than 30 fs. The very fast decay of the level is consistent with the width of the peak which is wider than 0.25 eV.[16,17]

3.3. Lifetimes of LUMO and LUMO+1. The molecule-derived LUMO and LUMO+1 levels are degenerate in a free molecule.[14,17] The degeneracy is lifted in the film, and the separate peaks labeled L0 and L1 appear, as shown in Figure 4 (see also the energy diagram in Figure 2b). The inset in Figure 4 shows the time evolution of the L0 peak intensity measured at RT and 30 K. The lifetime is evaluated to be 74 ± 4 fs with no clear temperature dependence. The weak temperature dependence suggests that phonons contribute only weakly to the decay process of the excited electron in L0. On the other hand, the dip between the L0 and L1 peaks becomes shallower at room temperature,[17] suggesting a phonon contribution to the bandwidth. The lifetimes around the L0 and L1 peaks measured at 30 K with the photon energy of 4.46 eV are shown in Figure 5, along with the 2PPE spectrum in Figure 4. The error bars in Figure 5 show day-to-day fluctuation. The increase in the lifetime at the leading edge of the L1 peak at 1.0 eV is in clear correspondence with the spectrum. A lifetime of 50 fs is observed for the small peak, L′, at 1.1 eV. The peak was left unassigned in our former paper.[17] The finite lifetime indicates that the peak arises from other split unoccupied components of the LUMO and LUMO+1. The contributions of the LUMO and LUMO+1 are large for the L0 and L1 levels, and these contributions are smaller than the substrate contribution for the L′ and L″ levels (see ref 17).

The origin of the L0 and L1 peaks, located at 0.71 and 0.87 eV above E_F, has been discussed in ref 17. Briefly, the peaks become stronger at photon energies above 4.09 eV because of the onset of resonant excitation from the occupied levels located at initial energies below −3.4 eV (HOMO-2 to -5). While the L1 peak is stronger than the L0 peak at photon energies between 4.18 and 4.28 eV, the L0 peak becomes stronger at photon energies above 4.38 eV. The inversion of the L0/L1 intensity ratio is due to the contribution of the resonant excitation to the L0 level from occupied levels below −3.7 eV (HOMO-6 to -8). The photon energy dependent intensity change indicates that the L0/L1 features arise from the resonance excitations from occupied levels due to HOMO-2 to HOMO-8 in the energy region between −3.4 and −4.0 eV. Excitation from the occupied σ band of the substrate, located below −4 eV initial energy, cannot explain the intensity changes. Population buildup in the L0/L1 levels by electron transfer from the substrate[27] is unlikely for the same reasons. The electron is located in the LUMO/LUMO+1-derived levels, and the hole is located in the HOMO-2 to -8 levels when the optical excitation occurs. The optically excited state is affected by hole scattering by substrate electrons,[17] and the hole is screened by substrate electrons. Because the hole is screened within the pulse width of the laser, the energies of the L0/L1 peaks are not largely affected by the detailed hole levels. The L0 and L1 peaks are well-separated. The separated peak shape can be simulated by a convolution with a Lorentzian function of 100 meV half width, while the rising edge of the L1 peak is sharper than the convoluted curve. Assuming that the peak width is determined by the lifetime of the hole, the lifetime is roughly estimated to be longer than 3 fs. The slight broadening of the peaks at RT suggests the shortening of the lifetime by about 10%. Ueno estimated the lifetime of the HOMO hole for pentacene/HOPG to be 2 fs.[4] Although the energies of the holes in HOMO-2 to -8 are higher than that in HOMO by 2−3 eV, the lifetimes are comparable to that of HOMO. The long lifetime may imply

that the excited electron elongates the hole lifetime than that of the bare hole. Thus the L0/L1 peaks represent the energy of electron in LUMO/LUMO+1 while the hole is screened. The energy separations between HOMO and the L0/L1 levels in our experiment are 2.04 and 2.20 eV, respectively (see Figure 2b).[14] The energy separations are larger than the lowest electronic excitation energy of 1.8 eV.[30] The large energy separations may be related to the absence of a hole in HOMO. It is interesting that the intensity ratio between the L0 and L1 peaks is nearly independent of the delay time. Decay from the L1 level to the lower-lying L0 level does not occur.

Several papers reported 2PPE spectroscopy for the lowest singlet excitonic state S_1 and the lowest triplet excitonic state T_1 in organic films.[27−29] The states were considered to be populated by relaxation from higher states. If S_1 and T_1 states of PbPc film can be populated by relaxation, 2PPE features other than the L0/L1 peaks should appear. Such a relaxation process is not clearly evident in our results. The relaxation may possibly be reflected in the shoulder at 0.4 eV (indicated by arrow in Figures 4 and 5) and in the sharply rising intensity at energy region below 0.3 eV in Figure 4. As for the PbPc film, the lifetimes at energies below 0.4 eV sharply increases from 90 fs to more than several picoseconds as the intermediate energy decreases. The lifetimes of the clean HOPG at the energy region depend on surface quality and typically change from 50 to 120 fs as the intermediate energy decreases from 0.4 to 0.1 eV. These values are similar to those in ref 31. The long lifetime for the PbPc film suggests that some molecule-derived unoccupied levels exist in the energy region. If the structures at energies below 0.4 eV are due to mixed contributions from the S_1, T_1 or other interface states,[28] the very long lifetime may be reasonable. The feature at energies below 0.3 eV seems rather similar to the spectral feature in ref 28, but detailed comparisons require further experiments.

AUTHOR INFORMATION

Corresponding Author

*E-mail: munakata@chem.sci.osaka-u.ac.jp. Phone: +81(0)6 6850 6082. Fax: +81(0)6 6850 5779.

ACKNOWLEDGMENT

This work was partly supported by a Grant-in-Aid for Scientific Research from JSPS (22350009). The authors are grateful to N. Ueno of Chiba University for supplying the PbPc sample, film preparation methods, and detailed information on his recent work.

REFERENCES

(1) Salaneck, W. R.; Seki, K.; Kahn, A.; Pireaux, J. J. *Conjugated Polymer and Molecular Interfaces*; Dekker: New York, 2002.
(2) Ishii, H.; Sugiyama, K.; Ito, E.; Seki, K. *Adv. Mater.* **1999**, *11*, 605.
(3) Sato, N.; Yoshida, H.; Tsutumi, K. *J. Mater. Chem.* **2000**, *10*, 85.
(4) Ueno, N.; Kera, S. *Prog. Surf. Sci.* **2008**, *83*, 490.
(5) Braun, S.; Salaneck, W. R.; Fahlman, M. *Adv. Mater.* **2009**, *21*, 1450.
(6) Muntwiler, M.; Yang, Q.; Tisdale, W. A.; Zhu, X.-Y. *Phys. Rev. Lett.* **2008**, *101*, 196403.
(7) Borisov, A. G.; Sametoglu, V.; Winkelmann, A.; Kubo, A.; Pontius, N.; Zhao, J.; Silkin, V. M.; Gauyacq, J. P.; Chulkov, E. V.; Echenique, P. M.; Petek, H. *Phys. Rev. Lett.* **2008**, *101*, 266801.
(8) Echenique, P. M.; Berndt, R.; Chulkov, E. V.; Fauster, Th.; Goldmann, A.; Höfer, U. *Surf. Sci. Rep.* **2004**, *52*, 219.
(9) Szymanski, P.; Garrett-Roe, S.; Harris, C. B. *Prog. Surf. Sci.* **2005**, *78*, 1.
(10) Heringdorf, F.-J. M.; Reuter, M.; Tromp, R. *Nature* **2001**, *412*, 517.
(11) Yamamoto, R.; Yamanoto, I.; Mikamori, M.; Yamada, T.; Miyakubo, K.; Munakata, T. *Surf. Sci.* **2011**, *605*, 982.
(12) Yamamoto, I.; Matsuura, N.; Mikamori, M.; Yamamoto, R.; Yamada, T.; Miyakubo, K.; Ueno, N.; Munakata, T. *Surf. Sci.* **2008**, *602*, 2232.
(13) Yang, A.; Shipman, S. T.; Garrett-Roe, S.; Johns, J.; Strader, M.; Szymanski, P.; Muller, E.; Harris, C. J. *Phys. Chem. C* **2008**, *112*, 2506.
(14) Yamamoto, I.; Mikamori, M.; Yamamoto, R.; Yamada, T.; Miyakubo, K.; Ueno, N.; Munakata, T. *Phys. Rev. B* **2008**, *77*, 115404.
(15) Munakata, T.; Shibuta, M.; Mikamori, M.; Yamada, T.; Miyakubo, K.; Sugiyama, T.; Sonoda, Y. *Proc. SPIE—Int. Soc. Opt. Eng.* **2006**, *6325*, 63250M.
(16) Shibuta, M.; Yamamoto, K.; Miyakubo, K.; Yamada, T.; Munakata, T. *Phys. Rev. B* **2009**, *80*, 113310.
(17) Shibuta, M.; Yamamoto, K.; Miyakubo, K.; Yamada, T.; Munakata, T. *Phys. Rev. B* **2010**, *81*, 115426.
(18) Schäfer, I.; Schlüter, M.; Skibowski, M. *Phys. Rev. B* **1987**, *35*, 7663.
(19) Lingle, R. L.; Ge, N.-H., Jr.; Jordan, R. E.; McNeill, J. D.; Harris, C. B. *Chem. Phys.* **1996**, *205*, 191.
(20) McNeill, J. D.; Lingle, R. L., Jr.; Jordan, R. E.; Padowitz, D. F.; Harris, C. B. *J. Chem. Phys.* **1996**, *105*, 3883.
(21) Berthold, W.; Rebentrost, F.; Feulner, P.; Höfer, U. *Appl. Phys. A: Mater. Sci. Process.* **2004**, *78*, 131.
(22) Hotzel, A.; Moos, G.; Ishioka, K.; Wolf, M.; Ertl, G. *Appl. Phys. B: Laser Opt.* **1999**, *68*, 615.
(23) Fauster, Th.; Weinelt, M.; Höfer, U. *Prog. Surf. Sci.* **2007**, *82*, 224.
(24) Knoesel, E.; Hotzel, A.; Wolf, M. *J. Electron Spectrosc. Relat. Phenom.* **1998**, *88−91*, 577.
(25) Vondrak, T.; Zhu, X.-Y. *J. Phys. Chem. B* **1999**, *103*, 3449.
(26) Kirchmann, P. S.; Loukakos, P. A.; Bovensiepen, U.; Wolf, M. *New J. Phys.* **2005**, *7*, 113.
(27) Varene, E.; Martin, I.; Tegeder, P. *J. Phys. Chem. Lett.* **2011**, *2*, 252.
(28) Dutton, G. J.; Jin, W.; Reutt-Robey, J. E.; Robey, S. W. *Phys. Rev. B* **2010**, *82*, 073407.
(29) Link, S.; Scholl, A.; Jacquemin, R.; Eberhardt, W. *Solid State Commun.* **2000**, *113*, 689.
(30) Salomon, E.; Papageorgiou, N.; Ferro, Y.; Layet, J. M. *Thin Solid Films* **2004**, *466*, 259.
(31) Moos, G.; Gahl, C.; Fasel, R.; Wolf, M.; Hertel, T. *Phys. Rev. Lett.* **2001**, *87*, 267402.